

Wavelet-Based Damage Detection Method for Beam-Like Structures

Hakan GÖKDAĞ^{1*}

¹*Uludağ University, Faculty of Engineering and Architecture, Department of Mechanical Engineering, 16059 Görükle Bursa Turkey*

Received: 25.03.2009 Revised: 18.11.2009 Accepted: 08.02.2010

ABSTRACT

This paper is concerned with a novel wavelet-based damage detection method for beam-like structures. The method employs the orthogonal wavelet transform (OWT), and is based on extracting an approximation function from the damaged mode of structure. This approximation function is considerably well correlated with the undamaged structural mode. Exploiting this function, the continuous wavelet transform (CWT) coefficients of both the damaged mode and the approximation function can be computed, and thus a reliable damage index can be obtained by taking their difference. The numerical simulations reveal that the proposed index is more capable in capturing damage-induced singularities than the classical approach based on using only the damaged mode.

Key Words: *Wavelet analysis, continuous wavelet transform, orthogonal wavelet transform, vibration modes, damage detection.*

1. INTRODUCTION

The wavelet analysis is an extremely sensitive tool to singularities in a signal. Many damage detection approaches have been developed so far by making use of this feature [1]. In this context, a number of methods have been developed to determine damage location and extent by wavelet transforming the spatial data such as mode shapes, static or dynamic displacement profiles. The main idea these methods are based on is that a local defect such as notch or crack gives rise to local stiffness loss, so that local discontinuities in the derivatives of data occur. If such a signal is wavelet transformed, the transform coefficients in the vicinity of defect appear to be peaks with relatively large magnitudes. Besides, a certain relation between damage extent and wavelet scale is reported at singularity point [2, 3].

It can easily be realized from the relevant literature that the work in the area of wavelet-based damage detection by spatial data can be divided into two main groups. The methods in the first group require only the damaged structural data [2-9]. Essentially, the CWT coefficients are computed and plotted for a particular scale or in scale-space domain to determine damage-induced

variations while the CWT coefficients of healthy structural data are also computed in the works of second group [10-12], and compared with the damaged ones. The comparison is mostly made by taking their difference or proportioning as in Ref. [12]. By the way, the method of Zhong and Oyadiji [13] can be placed in the intersection of these two groups. The authors subtract the wavelet coefficients of the undamaged part of beam from those of the damaged part, utilizing the symmetry or asymmetry of modes.

The first group has the advantage of not requiring healthy structural data, because this is generally not available. Moreover, finite element modeling may be difficult for some structures, so that undamaged data cannot be obtained numerically. However, a major drawback of these methods is that border distortion makes damage detection difficult, if damaged structural data is employed alone. Although several approaches such as extending data in the symmetric, asymmetric or periodic form, and by extrapolation [4, 9, 12, 14] have been introduced to diminish border effect, none of these can be used for every boundary type [14]. On the other hand, border

*Corresponding author, e-mail: hakangkd@uludag.edu.tr

distortion can be eliminated if healthy structural data is used as well. Additionally, damage signature becomes clearer when data size or damage extent decreases, if a reference data is available [13].

In this work, a novel wavelet-based damage detection method for beam type structures is proposed. The core of the approach is the extraction of a suitable approximation function from the damaged mode by the OWT, and using it as healthy mode. This method has the advantages of the previous two groups, i.e., only the damaged modes of beam are employed, but the variation of the suggested damage index is in good agreement with the one obtained by taking the difference of the CWT coefficients of damaged and healthy modes. Hence, this new index is highly sensitive to defect-induced singularities.

2. THEORY

2.1. The Basics of the Wavelet Transform

Let $\mathbf{L}^2(\square)$ denote square integral real space. Then, the CWT of a function $f(x) \in \mathbf{L}^2(\square)$ is defined as

$$W(a,b) = a^{-1/2} \int_{-\infty}^{\infty} f(x) \psi_{a,b}^*(x) dx, \quad a, b \in \square, \quad a > 0 \quad (1)$$

where $\psi_{a,b}(x)$ is derived from a mother wavelet $\psi(x) \in \mathbf{L}^2(\square)$ satisfying some other mathematical requirements, through the integers a and b , which are called as scale and shifting parameters. The relation is $\psi_{a,b}(x) = \psi((x-b)/a)$ [15]. In general $\psi(x)$ may be complex-valued, so the overstar indicates the complex conjugation. Eq.(1) is the convolution of $f(x)$ with the wavelet of scale a , so that $W(a,b)$ coefficient refers to the resemblance between them at the point b . At a discontinuity point $W(a,b)$ becomes comparatively large while its value is relatively lower at the smooth parts of $f(x)$.

The mother wavelet $\psi(x)$ is said to have N vanishing moments if $\int_{-\infty}^{\infty} \psi(x) x^m dx = 0$ is satisfied for the m values $m=0,1,\dots,N-1$. This feature is significant in capturing singularity points in data because the magnitude of $W(a,b)$ becomes larger at damage location as N rises while it has lower values at the intact parts of structure, and the transform becomes more stable. Hence, employing a wavelet with greater N is advantageous in revealing damage locations. However, the damage localisation deteriorates for larger N . Thus the trade-off between stability and localisation should be considered. In the earlier works such as Ref. [2] N was recommended to be at least two, if the vibration modes of beam were processed. Hence sym4, which has four vanishing moments, is employed in this work when computing the CWT-based damage indices.

The CWT is a redundant transformation since the parameters a and b are real numbers. Although this feature is useful for the purpose of damage identification, it is impractical for the signal representation with fewer

transform coefficients. The redundancy of the transform can be removed by selecting an orthogonal wavelet basis along with the dyadic sampling of a and b , i.e. $a = 2^m$, $b = n2^m$, where m and n are integers with $m \geq 0$. Then, the transform is called as the OWT. By the OWT $f(x)$ can be decomposed to the sum of the approximation function $A(x)$ at level m_0 , which represents the lower frequency content of $f(x)$, and the sum of detail functions $D_m(x)$ from minus infinitive up to the level m_0 as

$$f(x) = A_{m_0}(x) + \sum_{m=-\infty}^{m_0} D_m(x) \quad (2)$$

This type of representation is called as multi-resolution [15, 19].

2.2. The Proposed Damage Detection Method

The method is based on two primary assumptions, the first of which states that the damaged mode M_d can be assumed to be approximately equal to the sum of undamaged mode M_u and damage-induced local variations η , i.e. $M_d = M_u + \eta$ [13]. Furthermore, M_d and M_u may contain some noise due to the measurement if they are obtained experimentally or due to computational errors if they are obtained numerically. This noise can, in general, be random, having both higher and lower frequency parts. In addition, if M_d and M_u are obtained under the same conditions, they have likely the same amount of noise. When M_d is decomposed by the OWT regarding a suitable decomposition level (m) and a wavelet with enough vanishing moments, the extracted approximation function A is expected to be well-correlated with M_u , since lower frequency components are dominant in both of them. On the other hand, the beam span, on which modal data is measured, should not contain sudden cross-sectional variations, according to the second assumption. Because the A obtained in this case will be free of such local changes, so that M_u and A can not be compatible. Under these assumptions a suitable A which is very compatible with M_u can be extracted by the following steps:

I) In order to reduce border distortion M_d is first extended at the ends asymmetrically. Messina reports that this type of extension, he calls as *rotation*, outperforms others such as symmetric extension and cubic spline extrapolation [14], but produces poor results for built-in (cantilever) boundary. In this work, the beam with simply supported ends is considered, thus this extension is suitable. However, the method can be well applied when fixed end is extended appropriately. If M_d is of length l , then the length of the extended data is $3l$.

II) The OWT is defined for sequences with length of some powers of two [16], so the extended data is upsampled to the nearest power of 2 by the cubic spline interpolation.

III) This is the most significant step of the method. The suitable approximation function (A) is extracted from the extended and up-sampled data. To this end, a suitable wavelet and a proper N should be determined first. The wavelet family must constitute an orthogonal basis for the complete decomposition of signal, so the alternatives such as Daubechies, symlet, Coiflet, biorthogonal or reverse biorthogonal families [16] are considered. Among them the symlet family is selected in this work, since similar performances were experienced with the others. As to the N , it is known that the frequency spectrum of the scale function of wavelet shrinks about zero frequency, and becomes flatter when N increases [15, 17]. Then, the A extracted by such a wavelet will have lower frequency components, so that A and M_u can be expected to be well-correlated because M_u is free of damage effects. In addition, if high-frequency noise is of relatively small order, then the lower-frequency parts are dominant in M_u as well. When the Figure 3.15 in Ref.[15] is examined, one can realise that N should be between 10 and 20, since no significant change in wavelet spectrums occurs in this interval and for higher N values. Moreover, the higher N causes more computational errors [16]. Considering all these points sym15 was used in this study. In the second stage, the appropriate decomposition level (m) has to be determined. This requires some indices as the measure of how well A and M_u are correlated. In this context, examining the variations of the approximation energy ratio (Ea) along with MAC indices (MAC: Modal Assurance Criterion) between A and M_d with respect to decomposition level is proposed. Ea is defined as

$$Ea(\%) = 100 \frac{E_{A,m}}{E_{A,m} + E_{D,m}} \quad (3)$$

where $E_{A,m}$ denotes the energy of approximation coefficients at the m^{th} level, and $E_{D,m}$ stands for the sum of the energies of detail coefficients up to that level. It should be noted that these energies are computed by the sum of the squares of corresponding wavelet coefficients [15]. On the other hand, the MAC, which is widely employed in experimental modal analysis to indicate how well two modal data are compatible, is defined for the sequences $\{f_1\}$ and $\{f_2\}$ of length s as [18]

$$MAC(\{f_1\}, \{f_2\}) = \frac{(\{f_1\}^T \{f_2\})^2}{(\{f_1\}^T \{f_1\})(\{f_2\}^T \{f_2\})} \quad (4)$$

In addition to Ea , the variations of $MAC(M_d, A)$ and $MAC(M'_d, A')$, where $' = d/dx$, with respect to m are suggested to examine, which can be explained as follows: Damage effects, η , are assumed to be local. Moreover, if damage extents are of lower order, then M_d and M_u are expected to be extremely compatible such that one cannot distinguish one from the other by naked eye. Furthermore, we are interested in notch-type defects,

which cause curvature discontinuity at damage sites [2]. Thus, $MAC(M''_d, A'')$ and other MACs of higher derivatives are supposed to be lower while $MAC(M_d, A)$ and $MAC(M'_d, A')$ are expected to be very close to 1. Similarly, one may anticipate that $MAC(M_d, A)$ and $MAC(M'_d, A')$ are comparatively close to 1 for lower m , but they begin to decrease as m rises, since the more m rises the more high frequency noise components and damage-induced variations are removed from A , so that the correlation between them reduces. When the relation $a=2^m$ between scale and m is recalled, it is concluded that the magnitudes of decreases in $MAC(M_d, A)$ and $MAC(M'_d, A')$ will increase as m increases. It is possible to verify that the similar trend occurs in the variation of Ea . To sum up, with increasing m , $MAC(M_d, A)$, $MAC(M'_d, A')$, and Ea reduces, which in turn implies that the extracted A becomes more compatible with M_u . However, after a certain level the drop in these indices becomes remarkable, which indicates the A is no longer in agreement with M_u . Consequently, m has an upper limit; in other words there exists a threshold value m_t meaning that A is far from M_u , hence the decomposition levels satisfying $m < m_t$ must be regarded. If the variations of $MAC(M_d, A)$, $MAC(M'_d, A')$ and Ea in the range $0 < m < m_t$ are regarded, the highest drops in these indexes are observed at a certain level close to m_t . This indicates that the main components other than the damage and noise-induced contributions have begun to be removed from the approximation function. Hence, the previous one from that current level must be considered for the most suitable A , since this is the last level for damage and high frequency noise components to be eliminated from the approximation function.

IV) After extracting the suitable A , the index below can be used for damage detection [10, 11]

$$I_1 = |W_d - W_A| \quad (5)$$

where the subscripts d and A stand for M_d and A , respectively. To illustrate how well this index is compatible with the ideal case, another one defined as

$$I_2 = |W_d - W_u| \quad (6)$$

is computed as well, where u refers to M_u . In addition to the just aforementioned, the following index is also introduced to demonstrate to what extent I_1 is sensitive to damage:

$$I_3 = |W_d| \quad (7)$$

Before obtaining these indices, M_d , M_u , and A are extended asymmetrically to reduce boundary distortion.

3. NUMERICAL RESULTS

Consider the beam shown in Figure 1. Its length and cross-section dimensions are $L=1\text{m}$, $h=30\text{mm}$, b (width along z -axis)= 40mm . The material properties are E

(Young modulus)= 210GPa , ν (Poisson's ratio)= 0.33 , ρ (density)= 7850 kg/m^3 , respectively. The locations of notches are $L_1=0.3\text{m}$, $L_2=0.5\text{m}$, $L_3=0.9\text{m}$, and $h_i=26\text{mm}$, $l_i=1\text{mm}$ ($i=1,2,3$) for each damage. The first three vibration modes of the beam were obtained by ANSYS using the element BEAM188 (see Figure 2). The modes of the healthy beam were also found by the same model to obtain the index in Eq.(6).

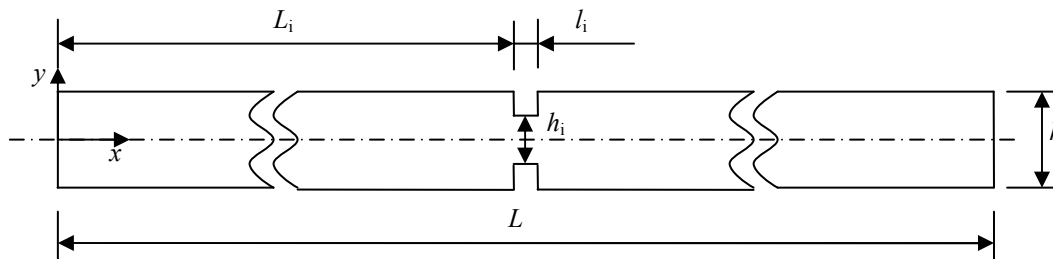


Figure 1. The beam and damage geometries.

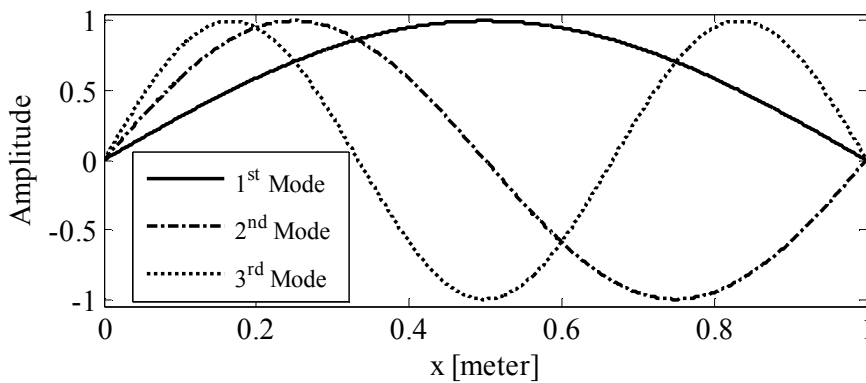


Figure 2. The first three vibration modes of the damaged beam.

Processing the first mode following the proposed scheme, Table 1 was obtained. According to the table, the 10th level should be discarded, since the approximation function is extremely far from resembling the undamaged mode at this level, as shown in Figure 3. This implies that the threshold is $m_t=10$. In this case, the interval $1 \leq m \leq 9$ must be regarded. In this interval it is observed that the maximum drop in the indices is recorded at the 9th level, thus the preceding level, i.e. $m = 8$, is the most suitable to obtain the approximation function. Then, the plots of indices in Eq.(5-7) come out as in Figure 4.

Figure 4 verifies that the proposed index I_1 is significantly compatible with I_2 , i.e. the ideal one. As expected, the wavelet modulus, i.e. the maxima of absolute values of wavelet coefficients, at a damage site form a cone of influence [19], which is an inherit feature of singularity point. Although damage signatures appear in I_3 plot as well, they are not as evident as in the graphs of I_1 and I_2 .

Table 1. The MACs and Ea for the first mode.

m (see Eq.(2))	$MAC(M_d, A)$	$MAC(M'_d, A')$	Ea
1	0.9999999998338	0.99999382398522	99.9999999881474
2	0.9999999996096	0.99998897289738	99.9999999674850
3	0.9999999994888	0.99998814958106	99.9999999560417
4	0.9999999994278	0.99998802792150	99.9999999503811
5	0.9999999993473	0.99998799919462	99.9999999488793
6	0.9999999993379	0.99998797155708	99.9999999407694
7	0.99999999937031	0.99998789407511	99.99999994367234
8	0.99999999765507	0.99998781557470	99.99999916887902
9	0.99999589606287	0.99998052397438	99.99998408142048
10	0.98205985453443	0.97590972312219	99.9983928433926

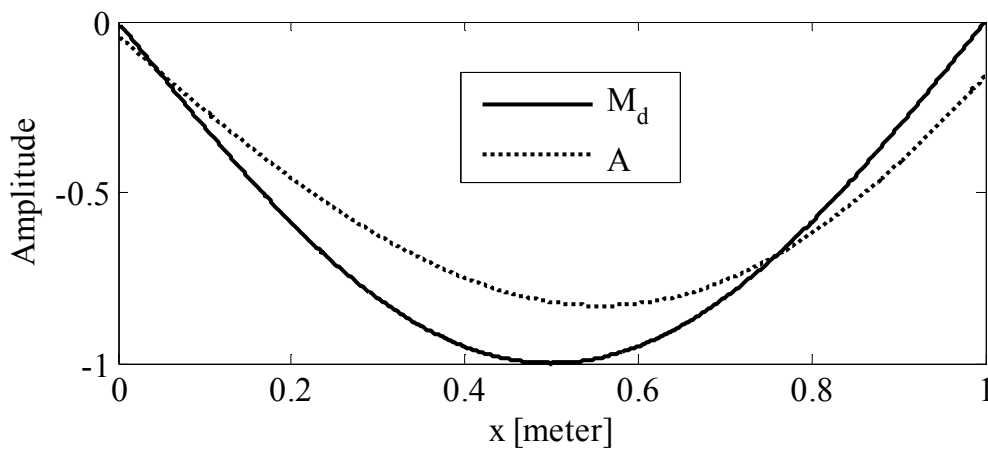
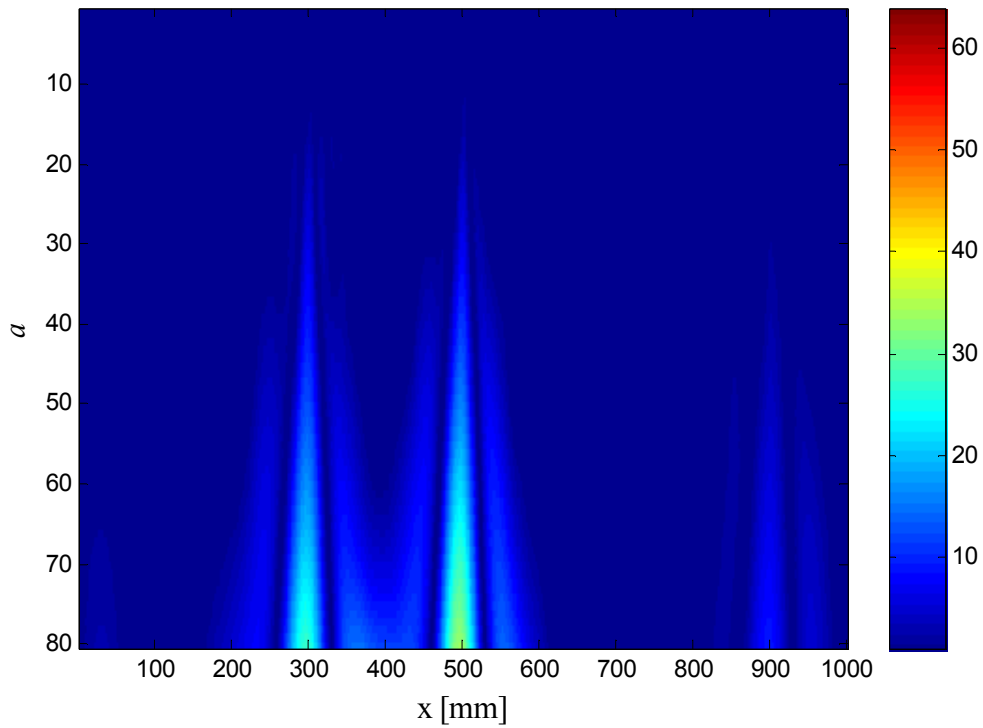
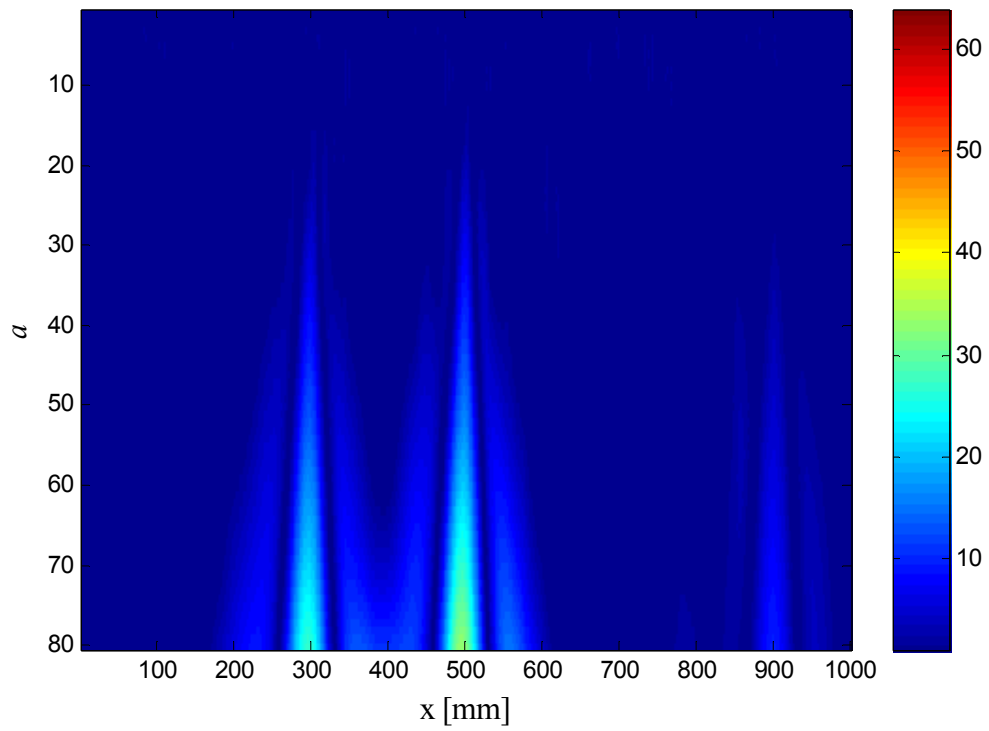


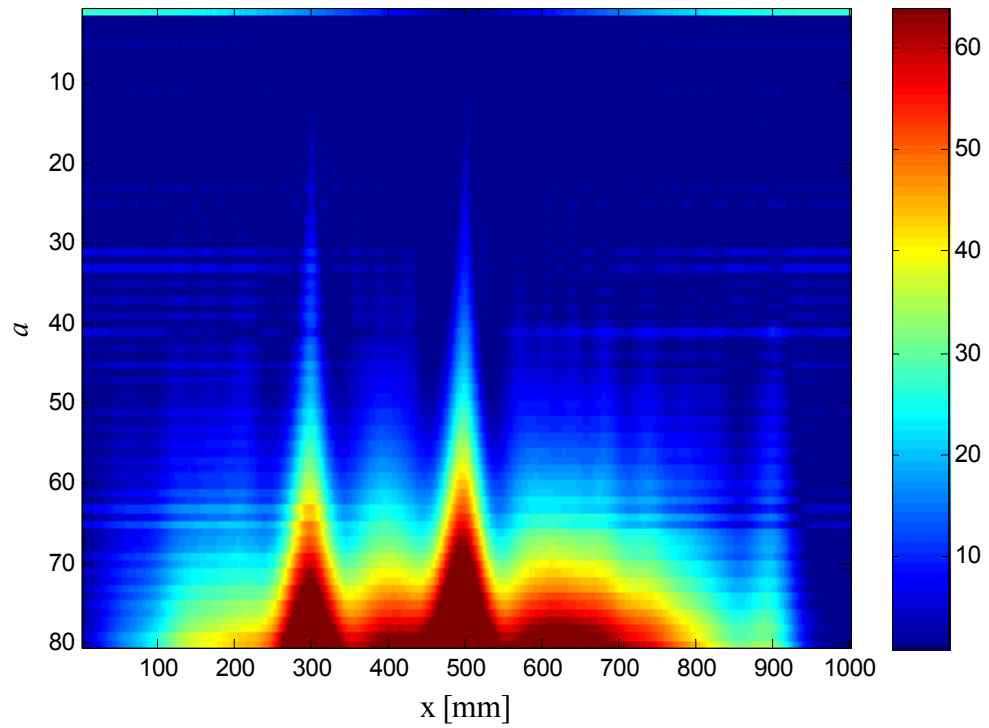
Figure 3. Comparison of the first damaged mode and the A at the 10th decomposition level. $MAC(M_d, A)=0.982$, $MAC(M'_d, A')=0.976$.



(a)

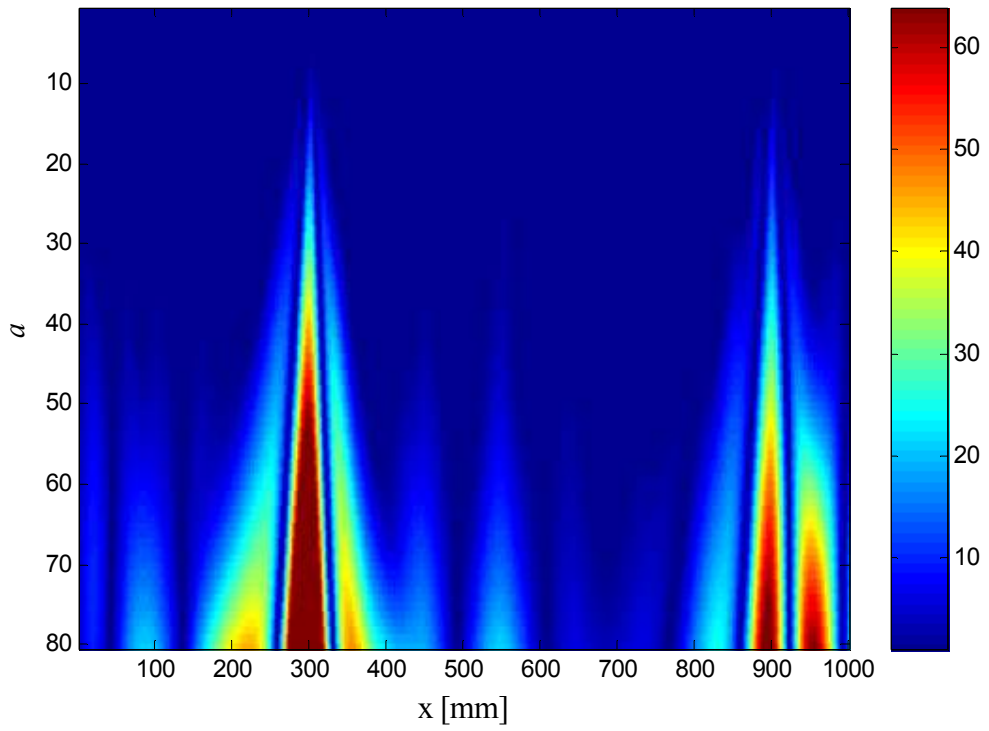


(b)

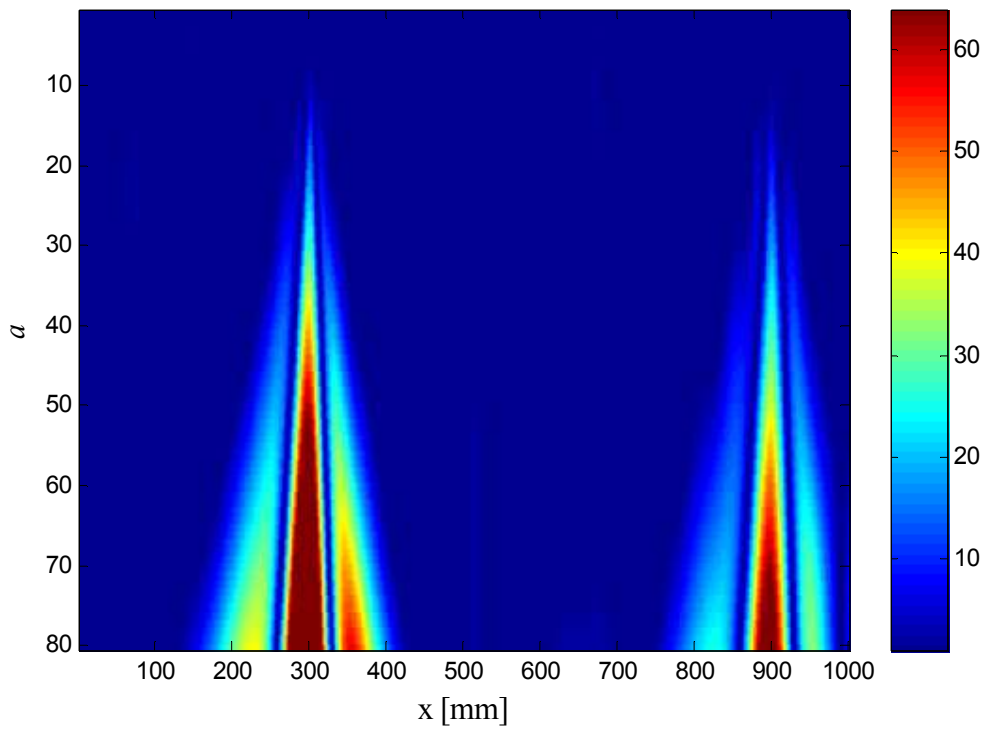


(c)

Figure 4. (a) $I_1 \times 10^5$, (b) $I_2 \times 10^5$, (c) $I_3 \times 10^5$, a : scale, the first mode is used.



(a)



(b)

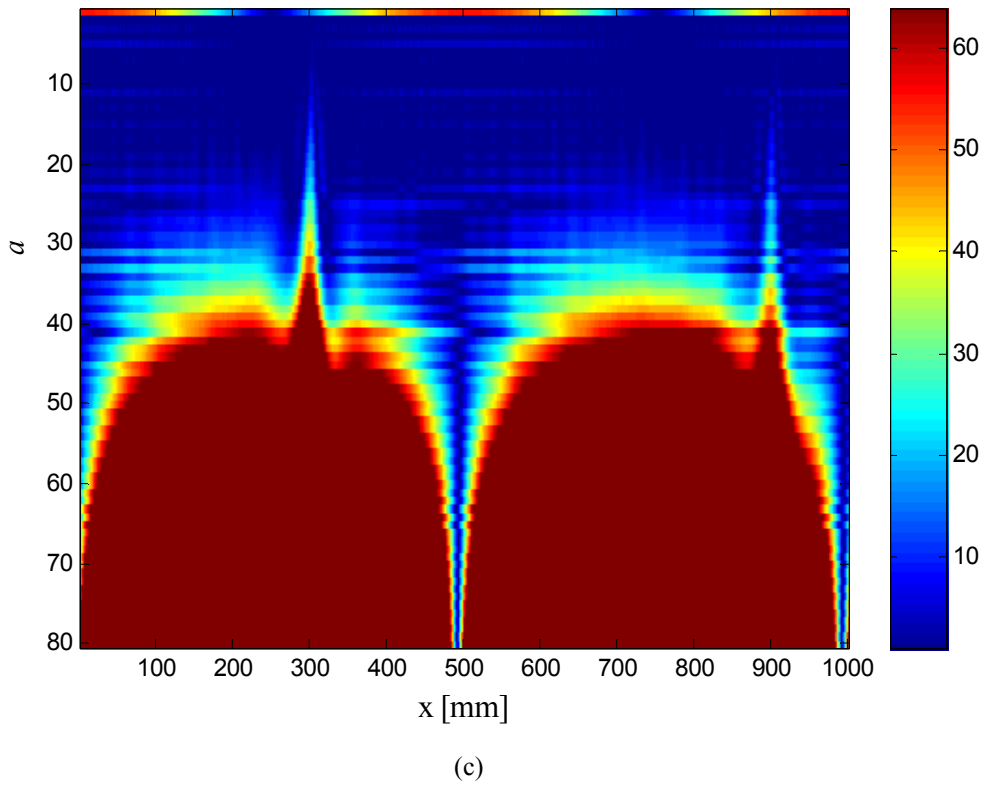


Figure 5. (a) $I_1 \times 10^5$, (b) $I_2 \times 10^5$, (c) $I_3 \times 10^5$, a : scale, the second mode is used.

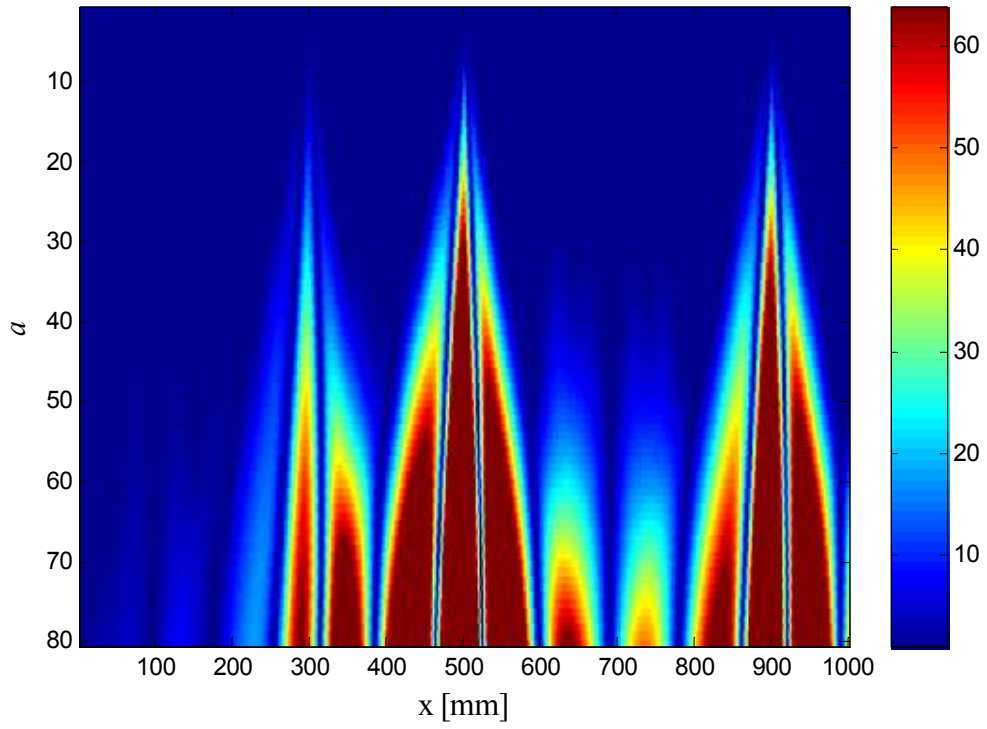
Since similar results were observed for the second mode, only Figure 5 is given here. The second damage is not perceived perfectly by this mode, since it is located at $x=0.5m$, the nodal point of that mode.

For the third mode, the indices change as in Table 2. The threshold is now $m_l = 9$, thus $1 \leq m \leq 8$ must be

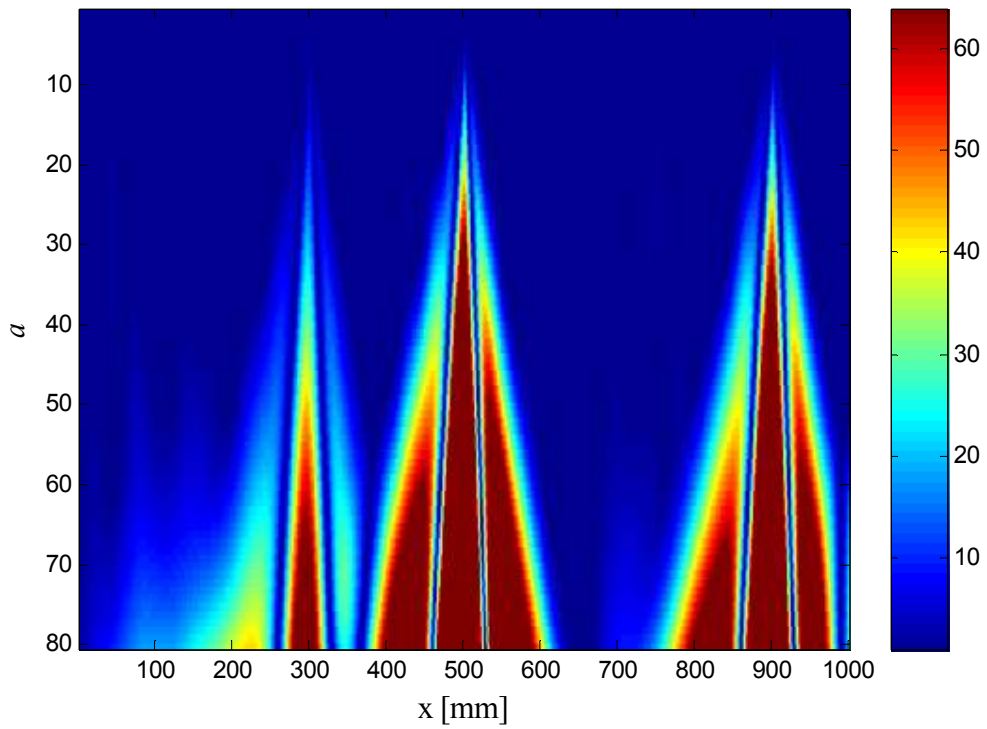
considered. In this interval, the first notable decrease in the indices is observed at the 8th level. Hence, the appropriate level for the approximation function is $m = 7$, and the corresponding plots are in Figure 6. Again, the results prove that the proposed method is very effective in identifying damage signatures.

Table 2. The MACs and Ea for the third mode.

m	$MAC(M_{d^r}A)$	$MAC(M'_{d^r}A')$	Ea
1	0.9999999997885	0.99999913755734	99.9999999858346
2	0.9999999995422	0.99999857545982	99.9999999620981
3	0.9999999993947	0.99999846384376	99.9999999469365
4	0.9999999988970	0.99999839534955	99.9999997730222
5	0.9999999963698	0.99999831104298	99.9999995887190
6	0.9999999683366	0.99999807772391	99.9999971811926
7	0.9999997485831	0.99999761327801	99.9999466930851
8	0.99994787125210	0.99963540985968	99.99983880272153
9	0.20108119287358	0.00438466607169	99.98106052696167
10	0.00196179216833	0.00148062583487	99.99595551914082



(a)



(b)

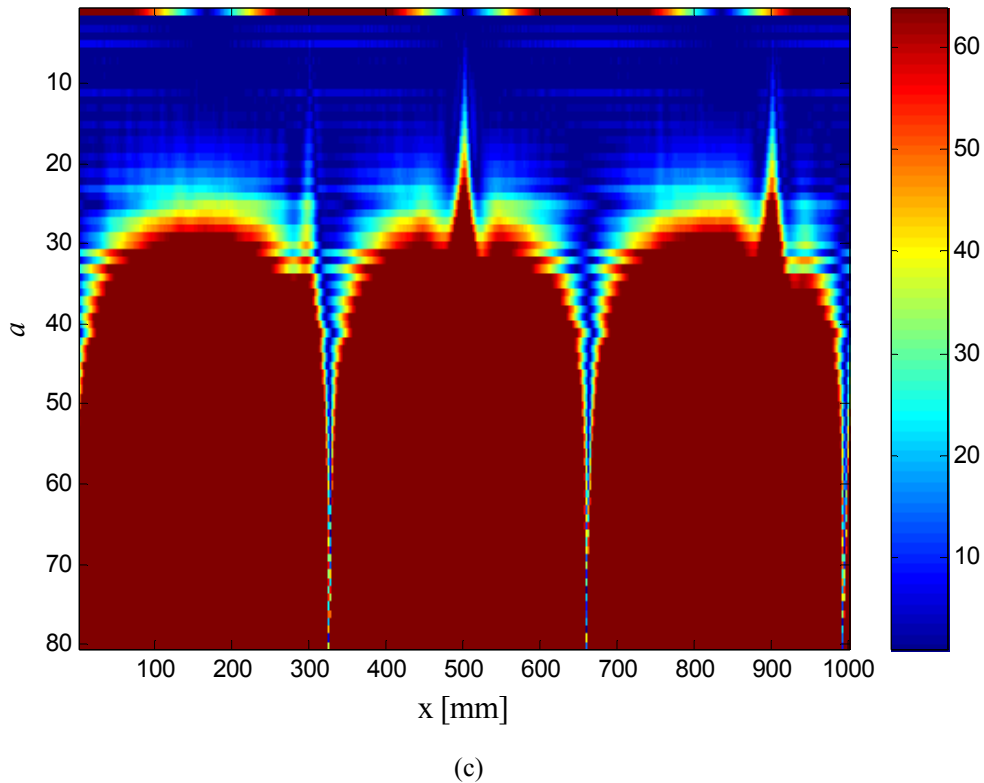


Figure 6. (a) $I_1 \times 10^5$, (b) $I_2 \times 10^5$, (c) $I_3 \times 10^5$, a : scale, the third mode is used.

4. CONCLUSIONS

A damage detection method based on the combination of the CWT and OWT is developed for beam-type structures. According to the previous publications, the difference of the CWT coefficients of healthy and damaged modes is a more capable index in revealing defect signature than only the CWT coefficients of damaged mode. Although the index proposed in this work uses only the damaged modes of beam, its performance is relatively close to the former. The capability of the method was illustrated through the numerical modes of a pinned-pinned beam. Although the results are not presented here due to limited place, it is also observed that it produces viable results for free boundary condition. Nevertheless, poor results are likely to come out when the method is applied to the beam with fixed end, because asymmetric extension is deficient in reducing border effect [14] for such boundary. However, if the fixed end is extended such that little border distortion occurs, then the method can well be applied. The future work will deal with the problem of dependency to border type and applying the method to two dimensional structures.

ACKNOWLEDGMENT

This work was carried out during the project 107M371 that was sponsored by TÜBİTAK.

REFERENCES

- [1] Kim, H., Melhem, H. "Damage detection of structures by wavelet analysis", *Engineering Structures*, 26: 347-62 (2004).
- [2] Hong, J.C., Kim, Y.Y., Lee, H.C., Lee, Y.W. "Damage detection using the Lipschitz exponent estimated by the wavelet transform: applications to vibration modes of a beam", *International Journal of Solids and Structures*, 39: 1803-16 (2002).
- [3] Douka, E., Loutridis, S., Trochidis, A. "Crack identification in beams using wavelet analysis". *International Journal of Solids and Structures*, 40: 3557-69 (2003).
- [4] Gentile, A., Messina, A., "On the continuous wavelet transforms applied to discrete vibrational data for detecting open cracks in damaged beams", *International Journal of Solids and Structures*, 40: 295-315 (2003).
- [5] Chang, C.C., Chen, L.-W. "Damage detection of a cracked thick rotating blades by a spatial wavelet based approach", *Applied Acoustics*, 65: 1095-111 (2004).
- [6] Chang, C.C., Chen, L.W. "Damage detection of a rectangular plate by spatial wavelet based approach", *Applied Acoustics*, 65: 819-32 (2004).

- [7] Loutridis, S., Douka, E., Trochidis, A. “Crack identification in double-cracked beams using wavelet analysis”, *Journal of Sound and Vibration*, 277: 1025-39 (2004).
- [8] Chang, C.C., Chen, L.W., “Detection of the location and size of cracks in the multiple cracked beam by spatial wavelet based approach”, *Mechanical Systems and Signal Processing*. 19: 139-55 (2005).
- [9] Rucka, M., Wilde, K., “Application of continuous wavelet transform in vibration based damage detection method for beams and plates”, *Journal of Sound and Vibration*, 297: 536-50 (2006).
- [10] Castro, E., Garcia-Hernández, M.T., Gallego, A., “Damage detection in rods by means of the wavelet analysis of vibrations: Influence of the mode order”, *Journal of Sound and Vibration*, 296: 1028-1038 (2006).
- [11] Castro, E., Garcia-Hernández, M.T., Gallego, A., “Defect identification in rods subject to forced vibrations using the spatial wavelet transform”, *Applied Acoustics*, 68: 699-715 (2007).
- [12] Zhu, X.Q., Law, S.S., “Wavelet-based crack identification of bridge beam from operational deflection time history”, *International Journal of Solids and Structures*, 43: 2299-2317 (2006).
- [13] Zhong, S., Oyadiji, S.O., “Crack detection in simply supported beams without baseline modal parameters by stationary wavelet transform”, *Mechanical Systems and Signal Processing*, 21: 1853-84 (2007).
- [14] Messina, A., “Refinements of damage detection methods based on wavelet analysis of dynamical shapes”, *International Journal of Solids and Structures*, 45: 4068-4097 (2008).
- [15] Addison, P.S., “The illustrated wavelet transform handbook: Introductory theory and applications in science, engineering, medicine and finance”, *IOP Publishing Ltd*, London, (2002).
- [16] Misiti, M., Misiti, Y., Oppenheim, G., Poggi, J.M., “Wavelet Toolbox 4 User’s Guide”, *The Mathworks, Inc*, (2007).
- [17] Debnath, L., “Wavelet transforms and their applications”,. Birkhäuser, Boston, (2002).
- [18] Ewins, D.J., “Modal testing: theory, practice and applications”, Baldock: Research Studies Press Ltd, (2000).
- [19] Mallat, S., “A wavelet tour of signal processing”. Academic Press, London, (1999).